# *Theoretical study on pure and doped $B_{12}N_{12}$ fullerenes as thiophene sensor*

**Elham Tazikeh-Lemeski, Alireza Soltani, Mohammad Taghi Baei, Masoud Bezi Javan & Sahar Moazen Rad**

**Adsorption**
Journal of the International Adsorption Society

ISSN 0929-5607
Volume 24
Number 6

Adsorption (2018) 24:585-593
DOI 10.1007/s10450-018-9965-y

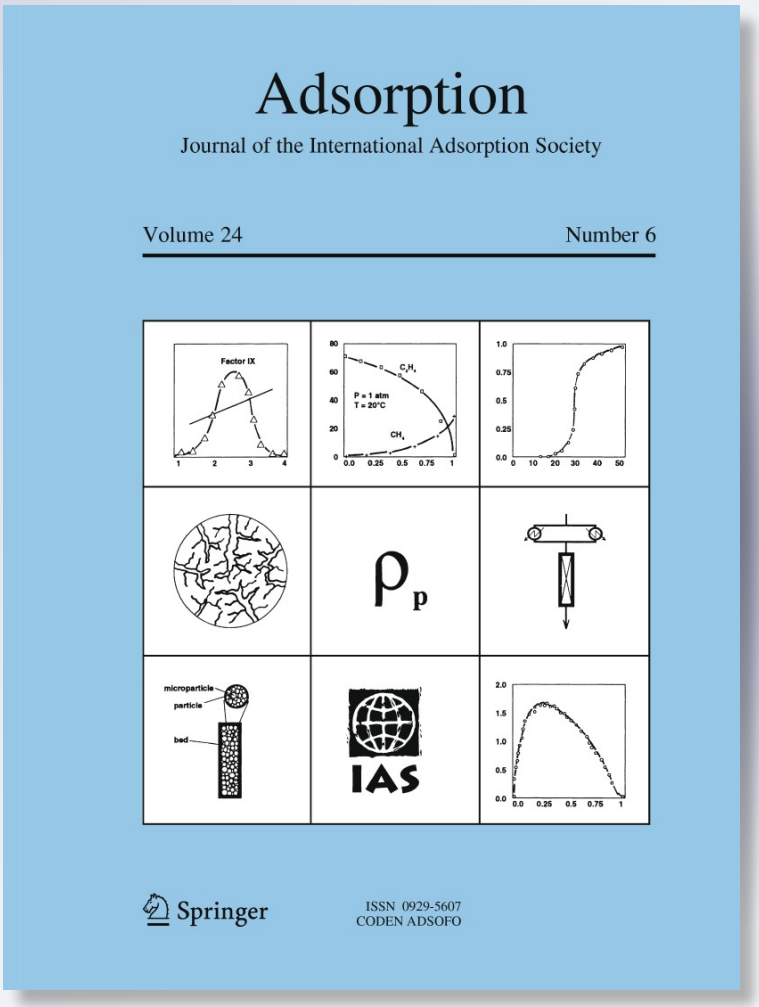


Springer

Adsorption (2018) 24:585–593
https://doi.org/10.1007/s10450-018-9965-y

# Theoretical study on pure and doped $B_{12}N_{12}$ fullerenes as thiophene sensor

**Elham Tazikeh-Lemeski[1] · Alireza Soltani[2] · Mohammad Taghi Baei[3] · Masoud Bezi Javan[4] · Sahar Moazen Rad[2]**

Received: 8 February 2018 / Revised: 7 May 2018 / Accepted: 30 July 2018 / Published online: 9 August 2018


**Abstract**
The physisorption and chemisorption of Thiophene ($C_4H_4S$) onto the $B_{12}N_{12}$, $B_{11}AlN_{12}$, and $B_{11}SiN_{12}$ fullerenes have been investigated in both gas and solvent environments by means of density functional theory calculation. We found that the higher physisorption of $C_4H_4S$ in the top site of boron atom of $B_{12}N_{12}$ fullerene is − 0.14 eV **(II)**, while in the top sites of Si and Al in $B_{11}AlN_{12}$ and $B_{11}SiN_{12}$ fullerenes were − 0.58 **(VII)** and − 1.08 eV **(V)**, respectively. We believe that $B_{11}AlN_{12}$ fullerene is responsible for the increase of binding energy and reduction of the energy band gap in comparison with $B_{11}SiN_{12}$ fullerene. This data demonstrates that the increase of charge transfer and dipole moment led to the accretion of binding energy. Therefore, $B_{11}AlN_{12}$ fullerene will give additional insights of reducing sulfur contents and it also can serve as an adsorbent in the detection of the $C_4H_4S$ molecule.

**Keywords** Density functional theory · Adsorption · Fullerene · Electronic structure · Vibrational frequency

## 1 Introduction

After the synthesis of BN fullerenes in 1998, these fullerene-like structures have attracted considerable attention due to their specific physical and chemical properties (Golberg et al. 1998; Stephan et al. 1998). BN fullerenes have excellent properties such as heat resistance in air, large band gaps, and structural stability (Paine and Narula 1990; Oku et al. 2000, 2001). As we know Boron is the only known element to form cage molecule clusters and their skeleton lattices such as $B_{12}$-icosalledron and tetragonal boron. In addition, because of the polar nature B–N bonds, BN nanostructures are expected to have higher reactivity than their Carbon analogise (Karttunen et al. 2008). In Particular, $B_{12}N_{12}$ fullerene has been theoretically devoted to the study of gas sensors (Baei 2013b; Esrafili and Nurazar 2014), biosensors (Shokuhi Rad and Ayub 2016b; Bezi Javan et al. 2016a; Wu et al. 2010), hydrogen storage (Shokuhi Rad and Ayub 2016c), and drug delivery (Bezi Javan et al. 2016b; Soltani et al. 2016). For example, theoretical studies clearly showed that the BN cluster could store $H_2$ molecules more readily than the carbon clusters (Bezi Javan et al. 2016b). Furthermore, based on calculated results, the $B_{12}N_{12}$ nanocage is expected to be a potential efficient adsorbent for the adsorption of toxic pyridine in environmental systems (Baei 2013c).

Thiophene or $C_4H_4S$ molecule, commonly called thiofuran, is known as a π-conjugated compound with a heteroatom that consisting of a flat 5-membered aromatic ring (Lu et al. 2001). In the past decade, the interaction between transition and none transition metal atoms with thiophene and its derivatives for the purpose of hydrodesulfurization (HDS) catalytic process and the removal of sulfur from petroleum fuels has been widely studied (Chen et al. 2004). Mills et al. reported the adsorption reactions of thiophene upon $Mo_2N/\gamma$–$Al_2O_3$ Catalysts using FT-IR spectroscopy (Wu et al. 2000). Recently, experimental studies indicated the reactive adsorption of thiophene on Ni/ZnO structure (Ryzhikov et al. 2008; Bezverkhyy et al. 2008; Zhang et al. 2012). Joshi et al. (2009) reported the $C_4H_4S$-binding energies for different sulfur-containing molecules on various Co–$MoS_2$ metal edge structures. Cheng

✉ Alireza Soltani
alireza.soltani46@yahoo.com; alireza.soltani@goums.ac.ir

[1] Department of Chemistry, Gorgan Branch, Islamic Azad University, Gorgan, Iran

[2] Golestan Rheumatology Research Center, Golestan University of Medical Sciences, Gorgan, Iran

[3] Department of Chemistry, Azadshahr Branch, Islamic Azad University, Azadshahr, Golestan, Iran

[4] Physics Department, Faculty of Sciences, Golestan University, Gorgan, Iran

et al. (2013) used density functional theory (DFT) calculations to study the adsorption of thiophene on icosahedral $Ni_{13}$ and Zn doped $Ni_{13}$ clusters. They concluded that thiophene is preferentially chemisorbed on $Ni_{13}$ and $Zn@Ni_{12}$ cages with the whole ring π-bond on the surface of the adsorbent. Denis and Iribarne (2010) investigated thiophene adsorption on Single Wall Carbon Nanotubes and graphene using the VDW-DF and LDA functionals. Recently by Peyghan et al., a study of adsorption of thiophene on the pristine (6, 0) AlN nanotubes was investigated in the gas phase using DFT calculations (Cristol et al. 2006). They demonstrated that the adsorption energies are based on the weak interaction between thiophene and the substrate. Nogueira and co-workers have shown that the CNTs loaded to thiophene groups amends the interaction between the substrates and a thiophene-derived polymer (Ahmadi Peyghan et al. 2013b). Baei et al. have theoretically investigated the adsorption of thiophene over $Zn_{12}O_{12}$ nanocage (Nogueira et al. 2007). Their results demonstrate that the thiophene is physically adsorbed on the surface of $Zn_{12}O_{12}$ nano-cage. Tuning the electronic structures of the $B_{12}N_{12}$ fullerenes for specific application is evident important in building specific electronic and mechanical devices. The functionalized or doped $B_{12}N_{12}$ fullerenes, which exhibit dramatic changes in electronic properties with respect to their pristine counterparts, further enlarge the application in nanomolecular range. Some kinds of sensors have been presented by different research groups. Wang et al. (2009) have theoretically shown that Si-doped boron nitride nanotubes (BNNTs) serving as a potential chemical sensor for HCN. Also, Al-doped graphenes are proposed as potential HCN sensor by Rastegar et al. (2013). Furthermore, Beheshtian et al. (2013) showed that unlike pristine aluminum nitride nanotubes (AlNNTs), the Al-rich AlNNT is a good strategy for improving the sensitivity of these tubes toward HCN molecules. The above results show that the doping is an appropriate method for improving the sensitivity of pristine nanotubes and nano-structured materials toward HCN molecules. On the other hand improving the sensing performance of pristine fullerenes toward various desired molecules through doping is too expensive. In the present study we attempted to find a high sensitive pristine nanostructured material for Thiophene detection in environmental systems without manipulating its structure. The objective of the present study is to study the interaction of Thiophene over the pure, $B_{11}AlN_{12}$, and $B_{11}SiN_{12}$ fullerenes through theoretical calculations performed within the formalism of density functional theory (DFT).

## 2 Computational details

All calculations were carried out by means of density functional theory (DFT) within the generalized-gradient approximation (GGA) (Baei 2013a) implemented in the Gaussian 03 program (Frisch et al. 2004). The revised version of Perdew, Burke, and Ernzerhof (PBE) exchange–correlation functional (Perdew et al. 1997) with polarization and diffuse functions 6-311+G** basis set is used in the study of pure, $B_{11}AlN_{12}$, and $B_{11}SiN_{12}$ fullerenes interacting with thiophene (Soltani et al. 2015a). Solvent effects were contained in the calculations via the PCM model, where the dielectric constant of water (ε = 78.4) was used. To calculate total energies, self-consistent field (SCF) and electron density calculations are performed with a convergence criterion of $1.0\times10^{-6}$ Hartree. In geometry optimizations, the cut-off values for force and displacement are 0.00045 Hartree/Bohr and 0.0018 Bohr, respectively. The optimized geometries of $B_{12}N_{12}$, $B_{11}AlN_{12}$, and $B_{11}SiN_{12}$ fullerenes are displayed in Fig. 1. Natural bond orbital (NBO) analysis was calculated by using PBE functional. Molecular electrostatic potential (MEP), Frontier molecular orbital (FMO) configurations were generated with the GaussView (GaussView 4 2004) program (Gaussian, Inc. Pittsburgh, PA). The corresponding adsorption energies ($E_{ad}$) of the mentioned systems were determined through the following equation:

$$E_{ad} = E_{C_4H_4S\text{-fullerene}} - \left(E_{adsorbent} + E_{fullerene}\right) \quad (1)$$

$$E_{ad} = E_{C_4H_4S\text{-doping-fullerene}} - \left(E_{C_4H_4S} + E_{doping\text{-}fullerene}\right) \quad (2)$$

where $E_{C_4H_4S/fullerene}$ and $E_{C_4H_4S/doping\text{-}fullerene}$ are the total energies of $C_4H_4S$ adsorbed upon $B_{12}N_{12}$, $B_{11}AlN_{12}$, and $B_{11}SiN_{12}$ fullerenes. $E_{C_4H_4S}$ is the total energy of the thiophene molecule. $E_{fullerene}$ and $E_{doping\text{-}fullerene}$ are the total energies of the $B_{12}N_{12}$, $B_{11}AlN_{12}$, and $B_{11}SiN_{12}$ fullerenes.

## 3 Results and discussion

Optimized geometries of all these structures, including the $C_4H_4S$, pure, and metal-doped $B_{12}N_{12}$ fullerenes were calculated by DFT calculations. The optimized geometries of the pure, $B_{11}AlN_{12}$, and $B_{11}SiN_{12}$ fullerenes indicate the B–N, Al–N, and Si–N bond lengths that belong to the 4-membered ring (4-MR) are 1.491, 1.847, and 1.814 Å, respectively. The MPA analysis represents that the electron charges with a value of 1.101 |e| for boron atoms and − 1.101 |e| for nitrogen atoms were uniformly distributed over the $B_{12}N_{12}$ fullerene with the $T_h$ symmetry. For $B_{11}AlN_{12}$ fullerene, the electron charges of Al, B, and N atoms are 0.557, 0.218, and − 0.157 |e|, while for $B_{11}SiN_{12}$ the electron charges of Si, B, and N atoms are found to be 1.120, 0.041, and − 0.378 |e|, respectively. This indicates that the Si site is more active than Al and B sites in the fullerene. Tables 1 and 2 present the weak physical adsorption of $C_4H_4S$ on the surface of $B_{12}N_{12}$ and also indicated that the electronic property of the fullerene is

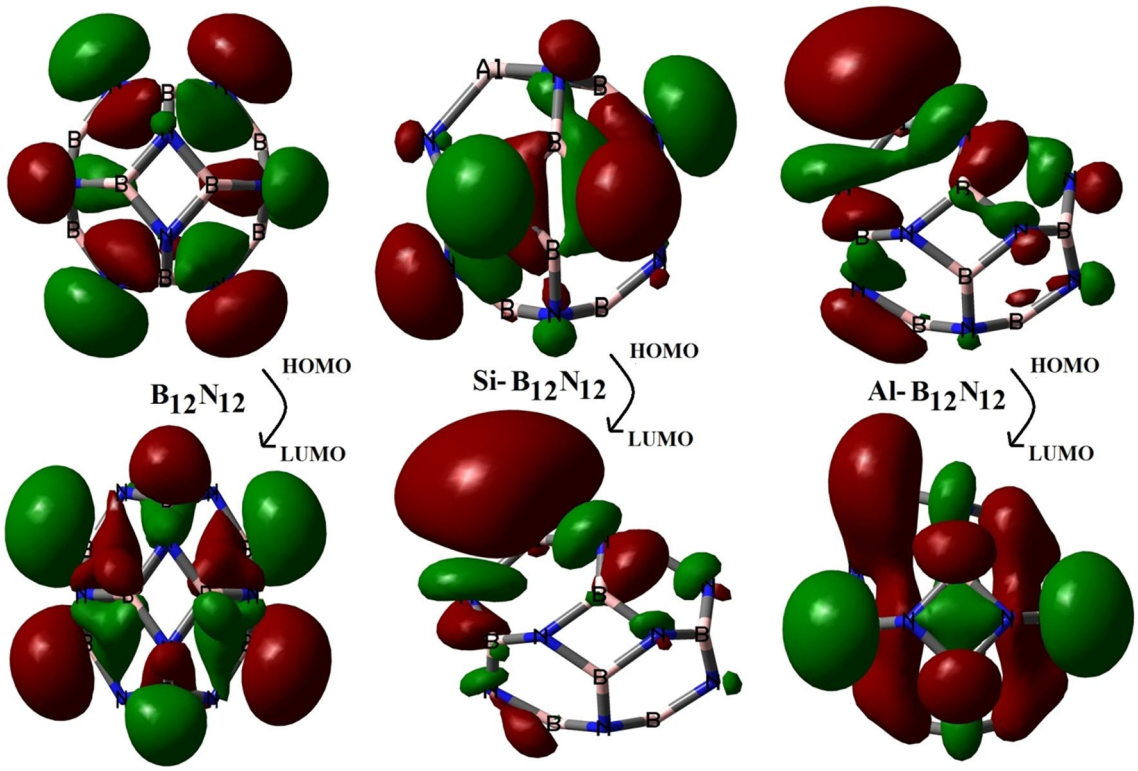


**Fig. 1** Frontier molecular orbital of pure and TM (Al/Si)-doped $B_{11}N_{12}$ fullerenes

sensitive to the presence of $C_4H_4S$. Our calculations reveal that the $E_{ad}$ of thiophene in the states **I** and **II** are found to be −0.13 and −0.14 eV and the distance between the molecule and the fullerene in the states **I** and **II** are 2.457 and 2.452 Å, respectively. We also calculated the solvation energy ($E_{solv}$) for the $C_4H_4S$ molecule interacting with $B_{12}N_{12}$ fullerene by the PBE functional. The discrepancy between these optimization energies equals to $E_{solv}$. The $E_{solv}$ values were calculated with the support of the 'Conductor-like Screening Model' for solvation (Andzelm and Kolmel 1995). A high negative value of $E_{solv}$ will give rise to a higher degree of solubility (Soltani et al. 2014a; Saikia and Deka 2010). The values of $E_{solv}$ for Thiophene adsorbed upon $B_{12}N_{12}$ fullerene in the states **I** and **II** is slightly increased to −0.16 and −0.17 eV in the water solution, respectively (See Table 2). As shown in Table 3, the thermodynamic parameters including Gibbs free energy changes (ΔG) and enthalpy changes (ΔH) at ambient pressure (P = 1 atm) and temperature (T = 298.14 K) are analyzed using the results of vibrational frequency calculations. The changes in ΔG and ΔH for the most stable state (**I**) became negative and the values of ΔG and ΔH were calculated to be −6.27 and −6.28 kcal/mol,

**Table 1** The binding energy, dipole moment ($\mu_D$/Debye), optimized geometrical parameters, HOMO–LUMO gaps $E_g$ (eV) for pure and TM (Al/Si)-doped $B_{11}N_{12}$ fullerenes in the gas phase

| Property | $E_{ad}$ (eV) | D (Å) | $E_{HOMO}$ (eV) | $E_{LUMO}$ (eV) | $E_g$ (eV) | $\Delta E_g$ (%) | $E_F$ (eV) | $\mu_D$ (Debye) |
|---|---|---|---|---|---|---|---|---|
| Thiophen | – | – | −5.86 | −1.40 | 4.46 | – | −3.63 | 0.47 |
| $B_{12}N_{12}$ | – | – | −7.03 | −2.04 | 4.99 | – | −4.54 | 0.0 |
| I | −0.13 | 2.457 | −6.45 | −2.49 | 3.96 | 20.64 | −4.47 | 3.91 |
| II | −0.14 | 2.455 | −6.47 | −2.50 | 3.97 | 20.44 | −4.49 | 3.95 |
| $B_{11}AlN_{12}$ | – | – | −6.63 | −3.76 | 2.87 | – | −5.20 | 3.37 |
| III | −0.91 | 2.482 | −5.97 | −3.39 | 2.58 | 10.10 | −4.68 | 10.1 |
| IV | −0.94 | 2.468 | −5.97 | −3.40 | 2.57 | 10.45 | −4.69 | 10.1 |
| V | −1.08 | 2.246 | −5.89 | −3.97 | 1.92 | 33.10 | −4.93 | 10.6 |
| $B_{11}SiN_{12}$ | – | – | −6.03 | −2.02 | 4.01 | – | −4.03 | 1.03 |
| VI | −0.48 | 3.305 | −5.64 | −1.95 | 3.69 | 7.98 | −3.80 | 2.65 |
| VII | −0.58 | 3.202 | −5.55 | −1.97 | 3.58 | 10.72 | −3.76 | 2.89 |

**Table 2** The binding energy, dipole moment ($\mu_D$/Debye), optimized geometrical parameters, HOMO–LUMO gaps $E_g$ (eV) for pure and TM (Al/Si)-doped $B_{11}N_{12}$ fullerenes in the solution phase

| Property | $E_{ad}$ (eV) | D (Å) | $E_{HOMO}$ (eV) | $E_{LUMO}$ (eV) | $E_g$ (eV) | $\Delta E_g$ (%) | $E_F$ (eV) | $\mu_D$ (Debye) |
|---|---|---|---|---|---|---|---|---|
| Thiophen | – | – | −5.94 | −1.48 | 4.46 | – | −3.71 | 0.48 |
| $B_{12}N_{12}$ | – | – | −6.98 | −1.94 | 5.04 | – | −4.46 | 0.0 |
| I | −0.16 | 2.201 | −6.42 | −2.59 | 3.83 | 24.0 | −4.51 | 7.42 |
| II | −0.17 | 2.198 | −6.45 | −2.59 | 3.86 | 23.4 | −4.52 | 7.46 |
| $B_{11}AlN_{12}$ | – | – | −6.61 | −3.28 | 3.33 | 33.9 | −4.95 | 5.63 |
| III | −1.02 | 2.412 | −6.18 | −2.78 | 3.40 | 2.10 | −4.48 | 14.39 |
| IV | −1.03 | 2.410 | −6.19 | −2.80 | 3.39 | 1.80 | −4.50 | 14.10 |
| V | −1.24 | 2.151 | −6.08 | −3.55 | 2.53 | 24.02 | −4.82 | 15.71 |
| $B_{11}SiN_{12}$ | – | – | −5.87 | −1.90 | 3.97 | 21.2 | −3.89 | 1.91 |
| VI | −0.11 | 3.244 | −5.33 | −1.90 | 3.43 | 13.6 | −3.62 | 4.27 |
| VII | −0.12 | 3.083 | −5.37 | −1.87 | 3.50 | 11.8 | −3.62 | 4.38 |

**Table 3** Thermodynamic parameters of Thiophene adsorbed on pure and TM (Al/Si)-doped $B_{12}N_{12}$ fullerenes in the most stable states at the water environment

| Property | ZPE | S | H | G | ΔS | ΔH | ΔG |
|---|---|---|---|---|---|---|---|
| $C_4H_4S$ | 40.53 | 68.23 | −552.61 | −552.64 | – | – | – |
| $B_{12}N_{12}$ | 78.13 | 98.58 | −955.04 | −955.08 | – | – | – |
| II | 118.86 | 129.78 | −1507.65 | −1507.73 | −37.03 | −6.28 | −6.27 |
| $B_{11}AlN_{12}$ | 75.01 | 102.58 | −1172.52 | −1172.57 | – | – | – |
| IV | 116.22 | 136.29 | −1725.17 | −1725.23 | −34.52 | −25.10 | −6.28 |
| V | 116.39 | 133.67 | −1725.17 | −1725.24 | −37.14 | −22.16 | −14.37 |
| $B_{11}SiN_{12}$ | 75.50 | 103.25 | −1219.54 | −1219.59 | – | – | – |
| VII | 116.24 | 142.07 | −1772.16 | −1772.23 | −29.41 | −3.34 | 4.46 |

respectively. The lower values of ΔG and ΔH imply that the adsorption process between two specious is not thermodynamically considerable. However, the low value of ΔG in comparison with ΔH is due to the entropic effect (Soltani et al. 2014d). Recently, the adsorption energy of thiophene via C=C bond on the zinc atom of $Zn_{12}O_{12}$ fullerene was found to be −0.42 eV using B3LYP/LANL2DZ level of theory (Cristol et al. 2006). The adsorption energy of thiophene via sulphur atom upon the surface of aluminium atom of AlN nanotube was calculated to be −0.87 eV using B3LYP/6-31G* level of theory (Cheng et al. 2013). In a study, Anota et al. (2015) calculated the adsorption energies of thiophene, benzothiophene, and dibenzothiophene on the surface of single wall armchair BN nanotube with the values of −0.49, −0.53, and −0.46 eV, respectively. The amount of dipole moment ($\mu_D$) after the interaction between molecule and fullerene increased to 3.91 Debye in the state **I** and 3.95 Debye in the state **II**, while the $\mu_D$ value for fullerene was zero. The low value of $\mu_D$ can result from the larger interaction distance and lower binding energy that is owed to a large vector in both systems (Soltani et al. 2018b). MPA analysis represents for states **I** and **II**, the charge transfers of 0.230 and 0.231 |e| occur from $C_4H_4S$ to the $B_{12}N_{12}$ fullerene. Based on MPA analysis after the $C_4H_4S$ adsorption on fullerene, the point charges over the B and S atoms were calculated to be 0.719 and −3.120 |e|, respectively, implying that the $C_4H_4S$ molecule function as an electron donor. This raised some questions: (1) Can the $C_4H_4S$ molecule alter the electronic properties of $B_{12}N_{12}$ fullerene? Based on the total density of states (TDOS), we noted that the adsorption of $C_4H_4S$ can be change the electronic property of both systems as changes of an energy gap ($\Delta E_g$) in the states **I** and **II** were 20.64 and 20.44%, respectively. When $C_4H_4S$ adsorbed over the surface of the adsorbent, the amount of $E_g$ was reduced to 3.96 eV (**I**) and 3.97 eV (**II**) compared with the pure fullerene (4.99 eV). Oku et al. experimentally reported that the energy band gap for $B_{12}N_{12}$ fullerene is 5.1 eV (Oku et al. 2004). Shokuhi Rad and Ayub have shown the energy band gap for $B_{12}N_{12}$ fullerene is 6.85 eV using B3LYP/6-31G** level of theory (Shokuhi Rad and Ayub 2016a). Baei et al. reported that the accuracy of PBE functional (in comparison with the B3LYP and PW91 functionals) is in good agreement with experimental data obtained by the Oku et al. (Baei 2013b). The $E_F$ of $B_{12}N_{12}$ fullerene is calculated to be approximately −4.535 eV. We found that the adsorption of $C_4H_4S$ can alter Fermi level energy ($E_F$) in states **I** (−4.470 eV) and **II** (−4.485 eV).

In the following, we investigated the effects of Al and Si doping on $B_{12}N_{12}$ fullerene that is replacing the B atoms of the fullerene during interaction with the $C_4H_4S$ molecule. Our results reveal that the Al and Si impurities can improve the binding energy and electronic properties of the fullerene

(Bahari et al. 2017; Ahmadi Peyghan et al. 2013a). Several studies have shown that the Al and Si-doped BN nanostructures can be improved the binding energy and electronic properties of the adsorption of different molecules (Baei et al. 2013; Ahmadi Peyghan et al. 2013c; Bahrami et al. 2013; Soltani et al. 2014b, c, 2015b). As can be seen in Fig. 1, the geometric structures of the $B_{11}AlN_{12}$ and $B_{11}SiN_{12}$ fullerenes are dramatically distorted, where the impurity Al and Si atoms out of the sidewall owing to its larger size than B atom. After the doping process, the Al-N and Si-N bond lengths were altered from 1.493 Å in free form to 1.847 and 1.814 Å, respectively, which is in good agreement with the results reported by other authors (Lin et al. 2015; Wang et al. 2008; Guerini et al. 2004; Esrafili et al. 2015; Baei et al. 2016; Vergara Reyes et al. 2018). The N–B–N and B–N–B angles in the 4-membered ring is about 98.48° and 80.15° and in the 6-membered ring is about 125.94° and 110.64°, respectively. For $B_{11}AlN_{12}$ and $B_{11}SiN_{12}$ fullerenes, the N–Al–N and N–Si–N angles in 4-membered rings are 83.25° and 81.93° and in 6-membered rings are 119.83° and 108.49°, respectively, which is smaller than the angle in the pure fullerene. Tables 2 and 3 demonstrate the strong adsorption of thiophene onto $B_{11}AlN_{12}$ in comparison with the pure and $B_{11}SiN_{12}$ fullerenes. In the case of Thiophene adsorption onto $B_{11}AlN_{12}$ fullerene, the value of binding energies in state **III, IV**, and **V** were found to be − 0.91, − 0.94, − 1.08 eV and the interaction distances are 2.482, 2.468, and 2.246 Å, respectively. As shown in Table 2, it is found that in going from gas environment to solvent environment, the $E_{ad}$ values increased to − 1.03, − 1.02, − 1.21 eV in the states **III, IV**, and **V**, respectively, and showed the interaction process between two specious in the states **V** is exothermic and thermodynamically feasible (ΔG = − 14.37 kcal/mol), compared to the state **VII** that is endothermic and thermodynamically unfavourable (ΔG = − 6.27 kcal/mol). In state **III** and **V**, the point charges of 0.405 and 0.393 |e| transferred from Thiophene to the adsorbent, respectively. Upon the adsorption of Thiophene onto $B_{11}AlN_{12}$ fullerene, the charges on the Al and S atoms were found to be − 0.815 and 0.339 (**III**), 0.018 and 0.201 (**IV**), − 0.598 and 0.321e (**V**). In the state **IV**, the point charges of Al, C, and S atoms are 0.018, − 0.309, and 0.201e, respectively, indicating that electron transfer of about 0.252 |e| from the $B_{11}AlN_{12}$ to Thiophene exists. The results obtained demonstrate in the state **IV**, $B_{11}AlN_{12}$ functions as an electron donor and the thiophene functions as an electron acceptor. The large distance in $B_{11}AlN_{12}$, causes a larger dipole moment owing to large vector, despite the fact that this results in a higher binding energy. As depicted in Fig. 1, the HOMO and LUMO orbitals are more localized on the nitrogen and boron atoms in $B_{12}N_{12}$ fullerene, respectively, whereas in $B_{11}AlN_{12}$ fullerene the HOMO orbitals are situated on the nitrogen atom and LUMO orbitals remains almost on the aluminum atom and nitrogen atoms near in doping site. For LUMO in Fig. 2II, the electrons are uniformly situated over $C_4H_4S$ molecule and the nitrogen atoms of fullerene, whereas for HOMO, the highest density of electrons is localized on the boron atoms near the interaction site. For the state **V**, the electron density distribution for HOMO is more situated on the aluminum and nitrogen atoms of the fullerene and the LUMO is more located on the $C_4H_4S$ molecule, whereas in the state **VII**, the HOMO and LUMO are more localized on the carbon and sulfur atoms of the molecule and the atoms of nitrogen and silicon of the fullerene. The computed MEP in Fig. 3 clearly reveals this interaction where the blue colour onto the adsorbed thiophene illustrates the positive charge (Abdolahi et al. 2018). We also investigated two different configurations of thiophene adsorbed on the $B_{11}SiN_{12}$ surface. For states **VI** and **VII**, the binding energies and interaction distances are found to be − 0.48 eV/3.305 Å and − 0.58 eV/3.202 Å, respectively. When Thiophene has a physical interaction onto $B_{11}SiN_{12}$ fullerene, the charges of about 0.009 and 0.054 |e| are transferred from fullerene to the Thiophene molecule.

To study effects of the Thiophene adsorption onto the electronic properties of the $B_{12}N_{12}$, $B_{11}AlN_{12}$, and $B_{11}SiN_{12}$ fullerenes, total density of states (TDOS) spectrum for all complexes were calculated (See Fig. 4). The energies of HOMO and LUMO in $B_{12}N_{12}$, $B_{11}AlN_{12}$, and $B_{11}SiN_{12}$ fullerenes are (− 7.03 and − 2.04 eV), (− 6.63 and − 3.76 eV), and (− 6.03 and − 2.02 eV), which give rise to an $E_g$ of 4.99, 2.87, and 4.01 eV in the gas phase, whilst the energies of HOMO and LUMO in water phase are (− 6.98 and − 1.94 eV), (− 6.61 and − 3.28 eV), and (− 5.87 and − 1.90 eV) since $E_g$ is altered from 5.04 eV in free form to 3.33 and 3.97 eV in $B_{11}AlN_{12}$ and $B_{11}SiN_{12}$ fullerenes, respectively. It is clear that $E_g$ of the $B_{11}SiN_{12}$ is higher (a band gap variation about 21.2%) than that of the $B_{11}AlN_{12}$ fullerene (a band gap variation about 33.9%). Based on the B3LYP/6-31G* level of theory, the energy gaps of the Al- and Si-doped $B_{11}N_{12}$ are found to be 4.26 and 5.77 eV, respectively (Baei et al. 2013). Baei et al. (2013) reported the value of $E_g$ in the $B_{12}N_{12}$ fullerene is reduced from 6.86 eV in the free form to 3.02 and 2.56 eV in the $Si_B$ and $Si_N$ models, respectively. After adsorption of Thiophene on $B_{11}AlN_{12}$, the HOMO and LUMO energies is slightly exalted with respect to those of $B_{11}AlN_{12}$ fullerene compared to $B_{11}SiN_{12}$ fullerene, as summarized in Table 1. The amount of $E_g$ for a single Thiophene is found to be 4.46 eV by the PBE functional, which is close to the calculated energy gap (4.99 eV) by Yu et al. (2015). The increment of the HOMO energy for $B_{11}AlN_{12}$ is vasty than that of the LUMO, so $E_g$ in this system is dropped from 2.87 eV to 2.58, 2.57, and 1.92 eV in the states **III, IV, V**, respectively. In contrast between the fullerenes, $B_{11}AlN_{12}$ indicates the high sensitivity to the presence of thiophene

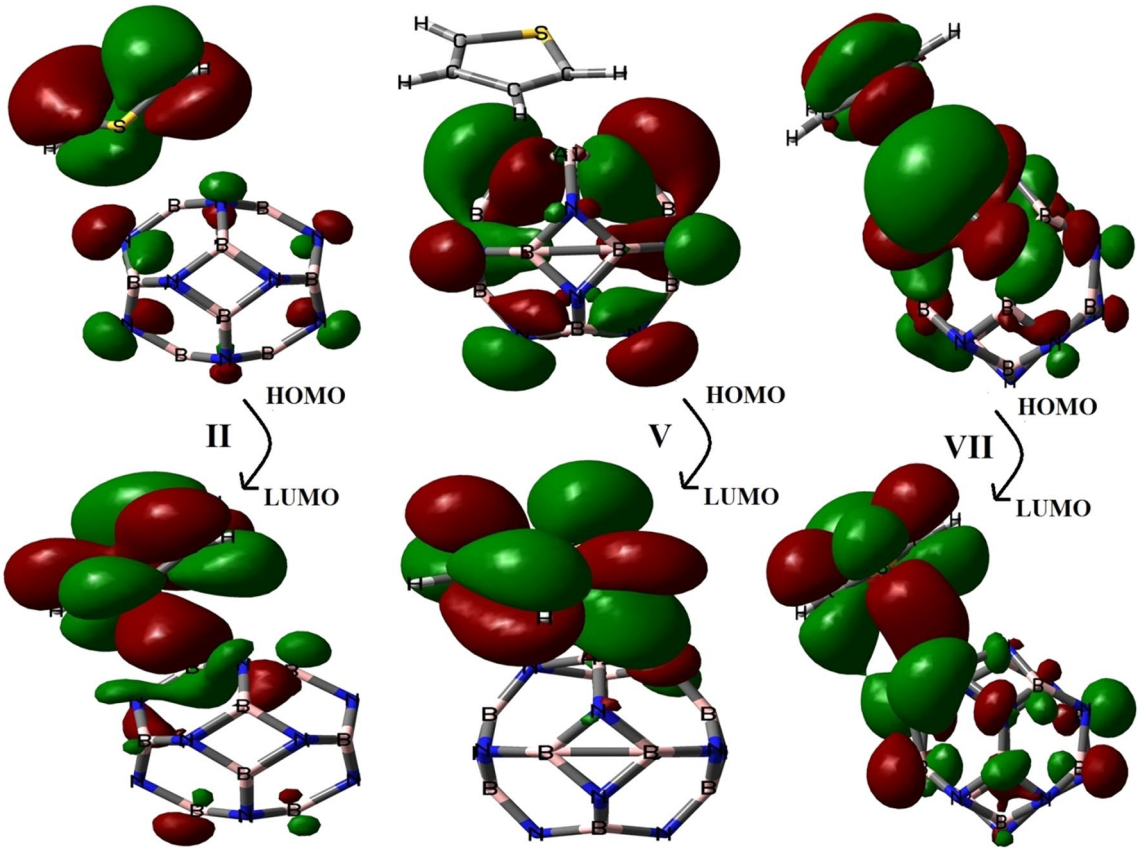


**Fig. 2** Frontier molecular orbital of thiophene adsorption over the pure and TM (Al/Si)-doped $B_{11}N_{12}$ fullerenes

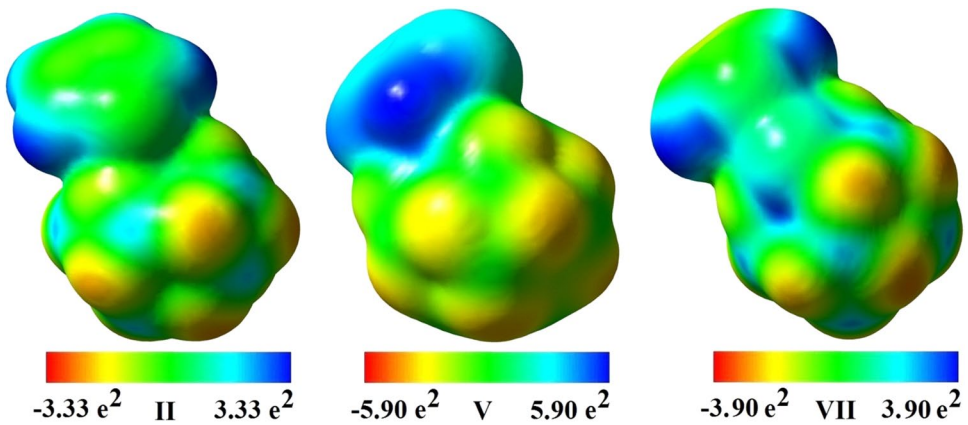


**Fig. 3** MEP of Thiophene adsorption over the pure and TM (Al/Si)-doped $B_{11}N_{12}$ fullerenes

while the change of energy gap ($\Delta E_g$) in the state **V** as the most stable state is about 33.10%, and for $B_{11}SiN_{12}$ in the state **VII** is $\Delta E_g = 10.72\%$.

Electron localization function (ELF) is a tool to characterize lone electron pairs and chemical bonds. The ELF given in Fig. 5 refers to the jellium-like homogeneous electron gas and renormalizes the value between 0.00 and 1.00. The values of 1.0 and 0.50 correspond to the perfect localization (red areas) and free electron gas behavior (green areas), respectively, whereas the ELF close to 0.00 corresponding to delocalized (Becke and Edgecombe 1990). As displayed in Fig. 5, ELF space contour plot indicates the interaction of $C_4H_4S$ molecule with the $B_{11}AlN_{12}$ fullerene and showed a high localization region between carbon atom and its bonding Al atom with the nature of chemical bonding (covalent bond) as the electron localization is very strong and the electrons freely distribute among the atoms (Cheng et al. 2013; Soltani et al. 2017).

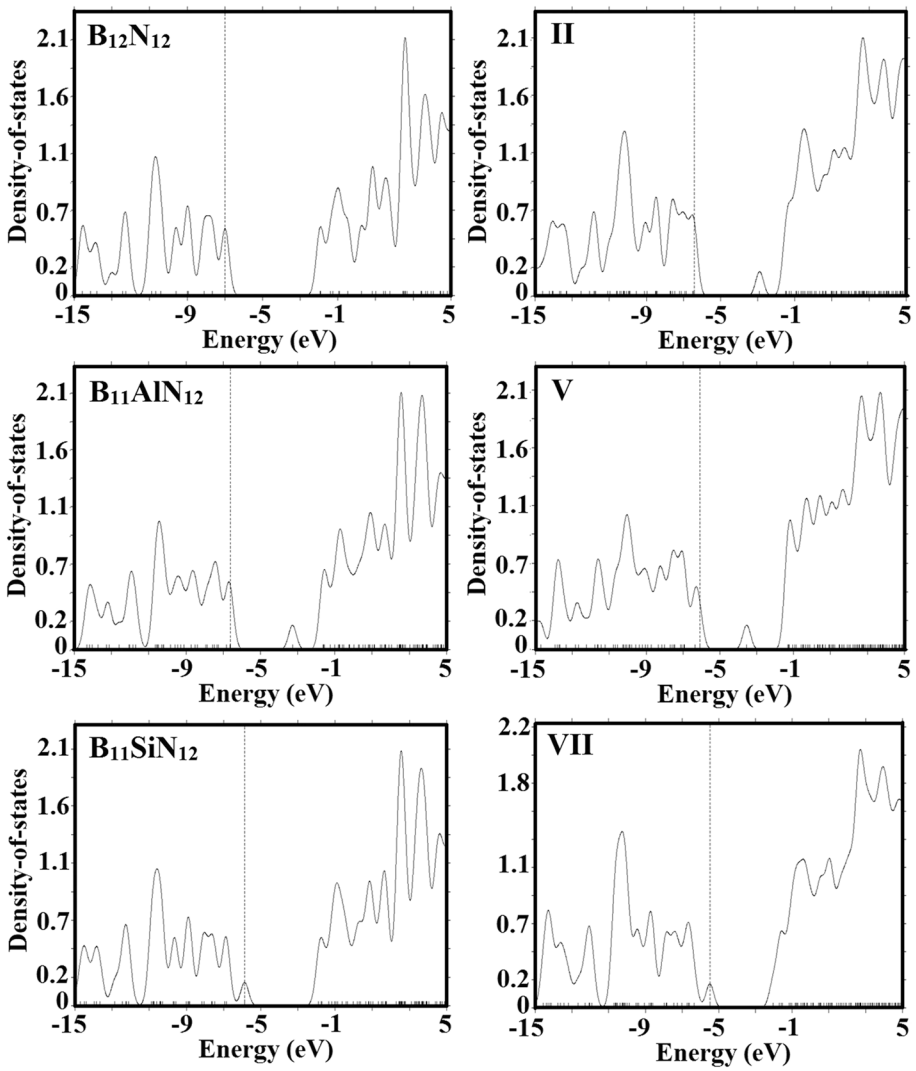


**Fig. 4** Calculated TDOS plots of Thiophene adsorbed over the pure and TM (Al/Si)-doped $B_{11}N_{12}$ fullerenes

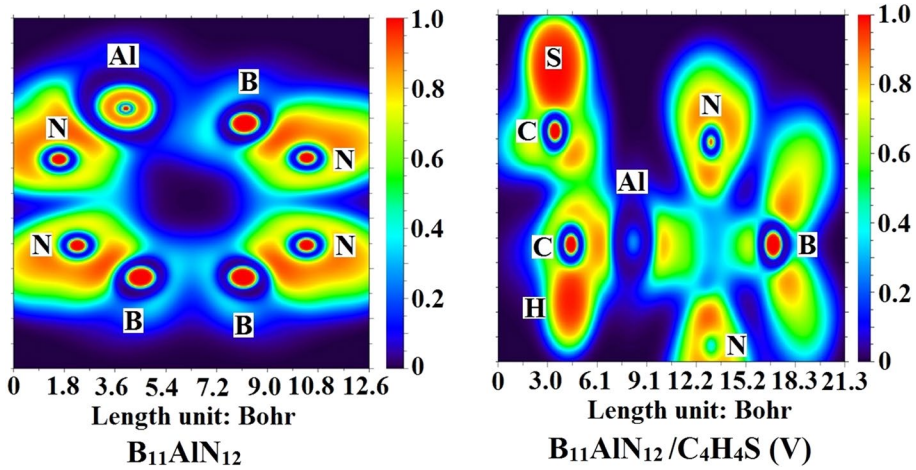


**Fig. 5** ELF plots of $B_{11}AlN_{12}$ and $B_{11}AlN_{12}/C_4H_4S$ complex

Based on infrared (IR) spectra the vibration frequencies of Thiophene adsorbed on the $B_{12}N_{12}$, $B_{11}AlN_{12}$, and $B_{11}SiN_{12}$ fullerenes in the water environment have been calculated by means of DFT. The calculated vibrational frequencies are in the range of 34–3195 $cm^{-1}$. We observed a strong band in region of 1413 $cm^{-1}$ is assigned to symmetric C=C

stretching vibration in free form of Thiophene. When Thiophene adsorbed upon $B_{12}N_{12}$ fullerene (**II**), a band at 1447 and 1538 $cm^{-1}$ is correspond to symmetric and asymmetry C=C stretching. The bands at around 731 and 822 $cm^{-1}$ are assigned to the symmetric vibrations of $C_4$–S and $C_1$–S, respectively, which is comparable to the results obtained by Yu and Liu (Yu et al. 2015; Liu et al. 2012). The IR spectra of Thiophene adsorbed exhibit a decrease in the symmetric and asymmetry C=C stretching vibrations calculated of the free molecule at 1422 and 1446 $cm^{-1}$ in the state **V** and 1449 and 1540 $cm^{-1}$ in the state **IV** for $B_{11}AlN_{12}$ fullerene and 1419 and 1509 $cm^{-1}$ in the state **VII** for $B_{11}SiN_{12}$ fullerene. This decreased stretching vibration can be attributed to the donation of the electrons of the $\pi$ system of the Thiophene to the bonds formed between the C atom of the molecule and the Al atom of the fullerene. The IR spectrum exhibits the band at 1421, 1361, and 1370 $cm^{-1}$, and is characteristic of B–N stretching in the $B_{12}N_{12}$, $B_{11}AlN_{12}$, and $B_{11}SiN_{12}$ fullerenes (Soltani et al. 2018a). Ayub et al. (2016) calculated that a band in the region of 1438 $cm^{-1}$ is assigned to the B-N stretching vibration, which is close to our calculations by PBE1 functional. The maximum band reported at 1365 $cm^{-1}$ is characteristic of B–N stretching vibration in the BNNTs by Samanta et al. (2010).

## 4 Concluding remarks

In conclusion, first principle theory based density functional theory calculations elucidate significantly the increased binding energy and dipole moment and decreased energy gap for thiophene interacting with $B_{11}AlN_{12}$ surface compared with the $B_{12}N_{12}$ and $B_{11}SiN_{12}$ fullerenes for both gas and water phases. It has been observed that the thiophene molecule strongly adsorbed with a significant charge transfer to the $B_{11}AlN_{12}$ surface. This lead to a large distortion on the substrate surface and broadened their $E_g$ significantly in comparison with the $B_{11}SiN_{12}$ fullerenes, which seems quite plausible for the detection of thiophene molecule. For same bonding state, the binding energy of Thiophene upon $B_{11}AlN_{12}$ is larger than that on $B_{12}N_{12}$ and $B_{11}SiN_{12}$ fullerenes, showing that there is an appreciable improves in the reactivity ability with an impurity TM atom in the fullerene.

**Acknowledgements** We thank the clinical Research Development Unit (CRDU), Sayad Shirazi Hospital, Golestan University of Medical Sciences, Gorgan, Iran.

## References

Abdolahi, N., Aghaei, M., Soltani, A., Azmoodeh, Z., Balakheyli, H., Heidari, F.: Adsorption of celecoxib on $B_{12}N_{12}$ fullerene: spectroscopic and DFT/TD-DFT study. Spectrochim. Acta A **204**, 348–353 (2018)

Ahmadi Peyghan, A., Hadipour, N., Bagheri, Z.: Effects of Al-doping and doubleantisite defect on the adsorption of HCN on a BC2N nanotube: DFT studies. J. Phys. Chem. C **117**, 2427–2432 (2013a)

Ahmadi Peyghan, A., Baei, M.T., Torabi, P., Hashemian, S.: Adsorption of thiophene on aluminum nitride nanotubes. Phosphorus Sulfur Silicon Relat. Elem. **188**, 1172–1177 (2013b)

Ahmadi Peyghan, A., Noei, M., Yourdkhani, S.: Al-doped graphene-like BN nanosheet as a sensor for para-nitrophenol: DFT study. Superlattices Microstruct. **59**, 115–122 (2013c)

Andzelm, J., Kolmel, C.: Incorporation of solvent effects into density functional calculations of molecular energies and geometries. J. Chem. Phys. **103**, 9312–9320 (1995)

Ayub, K.: Are phosphide nano-cages better than nitride nano-cages? A kinetic, thermodynamic and non-linear optical properties study of alkali metal encapsulated $X_{12}Y_{12}$ nano-cages. J. Mater. Chem. C **4**, 10919–10934 (2016)

Baei, M.T.: Covalent functionalization of $Zn_{12}O_{12}$ nanocluster with thiophene. J. Clust. Sci. **24**, 749–756 (2013a)

Baei, M.T.: $B_{12}N_{12}$ sodalite like cage as potential sensor for hydrogen cyanide. Comput. Theor. Chem. **1024**, 28–33 (2013b)

Baei, M.T.: Remove of toxic pyridine from environmental systems by using B12N12 nano-cage. Superlattices Microstruct. **58**, 31–37 (2013c)

Baei, M.T., Hashemian, S., Yourdkhani, S.: Silicon-doping makes the $B_{12}N_{12}$ insulator to an n or p-semiconductor. Superlattices Microstruct. **60**, 437–442 (2013)

Baei, M.T., Soltani, A., Hashemian, S.: Adsorption properties of hydrazine on pristine and Si-doped $Al_{12}N_{12}$ nano-cage. Phosphorus Sulfur Silicon Relat. Elem. **191**, 702–708 (2016)

Bahari, A., Jalalinejad, A., Bagheri, M., Amiri, M.: First principles study of electronic and structural properties of single walled zigzag boron nitride nanotubes doped with the elements of group IV. Solid State Commun. **267**, 1–5 (2017)

Bahrami, A., Seidi, S., Baheri, T., Aghamohammadi, M.: A first-principles study on the adsorption behaviour of amphetamine on pristine, P- and Al-doped $B_{12}N_{12}$ nano-cages. Superlattices Microstruct. **64**, 265–273 (2013)

Becke, A.D., Edgecombe, K.E.: A simple measure of electron localization in atomic and molecular systems. J. Chem. Phys. **92**, 5397–5403 (1990)

Beheshtian, J., Peyghan, A.A., Bagheri, Z.: Sensing behavior of Al-rich AlN nanotube toward hydrogen cyanide. J. Mol. Model. **19**(6), 2197–2203 (2013)

Bezi Javan, M., Soltani, A., Tazikeh Lemeski, E., Ahmadi, A., Moazen Rad, S.: Interaction of $B_{12}N_{12}$ nano-cage with cysteine through various functionalities: a DFT study. Superlattices Microstruct. **100**, 24–37 (2016a)

Bezi Javan, M., Soltani, A., Azmoodeh, Z., Abdolahi, N., Gholami, N.: A DFT study on the interaction between 5-fluorouracil and $B_{12}N_{12}$ nanocluster. RSC Adv. **6**, 104513–104521 (2016b)

Bezverkhyy, I., Ryzhikov, A., Gadacz, G., Bellat, J.-P.: Kinetics of thiophene reactive adsorption on Ni/$SiO_2$ and Ni/ZnO. Catal. Today **130**, 199–205 (2008)

Chen, J., Yang, H., Ring, Z.: HDS kinetics study of dibenzothiophenic compounds in LCO. Catal. Today **98**, 227–233 (2004)

Cheng, P., Zhang, S., Wang, P., Huang, S., Tian, H.: First-principles investigation of thiophene adsorption on $Ni_{13}$ and Zn@$Ni_{12}$ nanoclusters. Comput. Theor. Chem. **1020**, 136–142 (2013)

Chigo Anota, E., Cocoletzi, G.H., Garay Tapia, A.M.: Armchair Boron Nitride nanotubes-heterocyclic molecules interactions: a computational description. Open Chem. **13**, 734–742 (2015)

Cristol, S., Paul, J.-F., Schovsbo, C., Veilly, E., Payen, E.: DFT study of thiophene adsorption on molybdenum sulfide. J. Catal. **239**, 145–153 (2006)

Denis, P.A., Iribarne, F.: Thiophene adsorption on single wall carbon nanotubes and grapheme. J. Mol. Struct. (Thoechem.) **957**, 114–119 (2010)

Esrafili, M.D., Nurazar, R.: A density functional theory study on the adsorption and decomposition of methanol on $B_{12}N_{12}$ fullerene-like nanocage. Superlattices Microstruct. **67**, 54–60 (2014)

Esrafili, M.D., Saeidi, N., Nematollahi, P.: Can Si-embedded boron nitride nanotubes act as a favorable metal-free catalyst for CO oxidation by $N_2O$? RSC Adv. **5**, 100290–100298 (2015)

Frisch, M., Trucks, G., Schlegel, H., Scuseria, G., Robb, M., Cheeseman, J., et al.: Gaussian 03, revision D. 01. Gaussian Inc, Wallingford, CT (2004)

GaussView 4.1.2, Gaussian Inc., Wallingford, CT (2004)

Golberg, D., Bando, Y., Ste´phan, O., Kurashima, K.: Octahedral boron nitride fullerenes formed by electron beam irradiation. Appl. Phys. Lett. **73**, 2441–2443 (1998)

Guerini, S., Kar, T., Piquini, P.: Theoretical study of Si impurities in BN nanotubes. Eur. Phys. J. B **38**, 515–518 (2004)

Joshi, Y.V., Ghosh, P., Venkataraman, P.S., Delgass, W.N., Thomson, K.T.: J. Phys. Chem. C **113**, 9698–9709 (2009)

Karttunen, A.J., Linnolahti, M., Pakkanen, T.A.: Structural characteristics of perhydrogenated boron nitride fullerenes. J. Phys. Chem. C **112**, 10032–10037 (2008)

Lin, S., Ye, X., Huang, J.: Can metal-free silicon-doped hexagonal boron nitride nanosheets and nanotubes exhibit activity toward CO oxidation? Phys. Chem. Chem. Phys. **17**, 888–895 (2015)

Liu, D., Li, Z., Sun, Q., Kong, X., Zhao, A., Wang, Z.: In situ FT-IR study of thiophene adsorbed on the surface of sulfided Mo catalysts. Fuel **92**, 77–83 (2012)

Lu, X., Xu, X., Wang, N., Zhang, Q., Lin, M.C.: Chemisorption and decomposition of thiophene and furan on the Si(100)-2*1 surface: a quantum chemical study. J. Phys. Chem. B **105**, 10069–10075 (2001)

Nogueira, A.F., Lomba, B.S., Soto-Ovideo, M.A., Duarte Correia, C.R., Corio, P., Furtado, C.A., Hummelgen, I.A.: Polymer solar cells using single-wall carbon nanotubes modified with thiophene pedant groups. J. Phys. Chem. C **111**, 18431–18438 (2007)

Oku, T., Hirano, T., Kuno, M., Kusunose, T., Niihare, K., Suganuma, K.: Synthesis, atomic structures and properties of carbon and boron nitride fullerene materials. Mater. Sci. Eng. B **74**, 206–217 (2000)

Oku, T., Kuno, M., Kitahara, H., Nartia, I.: Formation, atomic structures, and properties of boron nitride and carbon nanocage fullerene materials. Int. J. Inorg. Mater. **3**, 597–612 (2001)

Oku, T., Nishiwaki, A., Narita, I.: Formation and atomic structure of $B_{12}N_{12}$ nanocage clusters studied by mass spectrometry and cluster calculation. Sci. Technol. Adv. Mater. **5**, 635–638 (2004)

Paine, R.T., Narula, C.K.: Synthetic routes to boron nitride. Chem. Rev. **90**, 73–91 (1990)

Perdew, J.P., Burke, K., Ernzerhof, M.: Generalized gradient approximation made simple. Phys. Rev. Lett. **78**, 1396 (1997)

Rastegar, S.F., Ahmadi Peyghan, A., Hadipour, N.L.: Response of Si- and Al-doped graphenes toward HCN: a computational study. Appl. Surf. Sci. **265**, 412–417 (2013)

Ryzhikov, A., Bezverkhyy, I., Bellat, J.-P.: Reactive adsorption of thiophene on Ni/ZnO: role of hydrogen pretreatment and nature of the rate determining step. Appl. Catal. B **84**, 766–772 (2008)

Saikia, N., Deka, R.C.: Theoretical study on pyrazinamide adsorption onto covalently functionalized (5,5) metallic single-walled carbon nanotube. Chem. Phys. Lett. **500**, 65–70 (2010)

Samanta, S.K., Gomathi, A., Bhattacharya, S., Rao, C.N.R.: Novel nanocomposites made of boron nitride nanotubes and a physical gel. Langmuir **26**(14), 12230–12236 (2010)

Shokuhi Rad, A., Ayub, K.: Adsorption of pyrrole on $Al_{12}N_{12}$, $Al_{12}P_{12}$, $B_{12}N_{12}$, and $B_{12}P_{12}$ fullerene-like nano-cages; a first principles study. Vacuum **131**, 135–141 (2016a)

Shokuhi Rad, A., Ayub, K.: A comparative density functional theory study of guanine chemisorption on $Al_{12}N_{12}$, $Al_{12}P_{12}$, $B_{12}N_{12}$, and $B_{12}P_{12}$ nano-cages. J. Alloys Compd. **762**, 161–169 (2016b)

Shokuhi Rad, A., Ayub, K.: Enhancement in hydrogen molecule adsorption on $B_{12}N_{12}$ nano-cluster by decoration of nickel. Int. J. Hydrog. Energy **41**, 22182–22191 (2016c)

Soltani, A., Baei, M.T., Tazikeh Lemeski, E., Shahini, M.: Sensitivity of BN nano-cages to caffeine and nicotine molecules. Superlattices Microstruct. **76**, 315–325 (2014a)

Soltani, A., Baei, M.T., Tazikeh Lemeski, E., Allah, A., Pahlevani: The study of $SCN^-$ adsorption on $B_{12}N_{12}$ and $B_{16}N_{16}$ nano-cages. Superlattices Microstruct. **75**, 716–724 (2014b)

Soltani, A., Baei, M.T., Ghasemi, A.S., Tazikeh Lemeski, E., Hosseni Amirabadi K.: Adsorption of cyanogen chloride over Al- and Ga-doped BN nanotubes. Superlattices Microstruct. **75**, 564–575 (2014c)

Soltani, A., Baei, M.T., Mirarab, M., Sheikhi, M., Tazikeh, E., Lemeski: The electronic and structural properties of BN and BP nano-cages interacting with $OCN^-$: a DFT study. J. Phys. Chem. Solids **75**, 1099–1105 (2014d)

Soltani, A., Bezi, M., Javan: Carbon monoxide interactions with pure and doped $B_{11}XN_{12}$ (X = Mg, Ge, Ga) nano-clusters: a theoretical study. RSC Adv. **5**, 90621–90631 (2015a)

Soltani, A., Baei, M.T., Tazikeh Lemeski, E., Kaveh, S., Balakheyli, H.: A DFT study of 5-fluorouracil adsorption on the pure and doped BN nanotubes. J. Phys. Chem. Solids **86**, 57–64 (2015b)

Soltani, A., Sousaraei, A., Bezi Javan, M., Eskandari, M., Balakheyli, H.: Electronic and optical properties of 5-AVA functionalized BN nanoclusters: a DFT study. N. J. Chem. **40**, 7018 (2016)

Soltani, A., Bezi Javan, M., Hoseininezhad-Namin, M.S., Tajabord, N., Tazikeh Lemeski, E., Pourarian, F.: Interaction of hydrogen with Pd- and Co-decorated $C_{24}$ fullerenes: density functional theory study. Synth. Met. **234**, 1–8 (2017)

Soltani, A., Ramezani Taghartapeh, M., Erfani-Moghadam, V., Bezi Javane, M., Heidari, F., Aghaei, M., Mahon, P.J.: Serine adsorption through different functionalities on the $B_{12}N_{12}$ and Pt-$B_{12}N_{12}$ nanocages. Mater. Sci. Eng. C **92**, 216–227 (2018a)

Soltani, A., Bezi Javan, M., Baei, M.T., Azmoodeh, Z.: Adsorption of chemical warfare agents over $C_{24}$ fullerene: effects of decoration of cobalt. J. Alloys Compd. **735**, 2148–2161 (2018b)

Stephan, O., Bando, Y., Loiseau, A., Willaime, F., Shramchenko, N., Tamiya, T., Sato, T.: Formation of small single-layer and nested BN cages under electron irradiation of nanotubes and bulk material. Appl. Phys. A **67**, 107–111 (1998)

Vergara Reyes, H.N., Chigo Anota, E., Castro, M.: $C_{60}$-like boron carbide and carbon nitride fullerenes: stability and electronic properties obtained by DFT methods. Fuller. Nanotub. Carbon Nanostruct. **26**, 52–60 (2018)

Wang, R., Zhu, R., Zhang, D.: Adsorption of formaldehyde molecule on the pristine and silicon-doped boron nitride nanotubes. Chem. Phys. Lett. **467**, 131–135 (2008)

Wang, R., Zhang, D., Liu, Y., Liu, C.: A theoretical study of silicon-doped boron nitride nanotubes serving as a potential chemical sensor for hydrogen cyanide. Nanotechnology **20**, 505704(1)–505704(8) (2009)

Wu, Z., Li, C., Wei, Z., Ying, P., Xin, Q.: FT-IR Spectroscopic studies of thiophene adsorption and reactions on $Mo_2N/\gamma$-$Al_2O_3$ catalysts. J. Phys. Chem. B **104**, 3237 (2000)

Wu, H.Y., Fan, X.F., Kuo, J.-L., Deng, W.-Q.: Carbon doped boron nitride cages as competitive candidates for hydrogen storage materials. Chem. Commun. **46**, 883–885 (2010)

Yu, T., Cheng, P., Huang, S., Wang, P., Tian, H.: First-principle investigation of thiophene adsorption on TM (Ni/Co/Mn)-doped $(ZnO)_{15}$ nanotube. Comput. Theor. Chem. **1057**, 15–23 (2015)

Zhang, Y., Yang, Y., Han, H., Yang, M., Wang, L., Zhang, Y., Jiang, Z., Li, C.: Ultra-deep desulfurization via reactive adsorption on Ni/ZnO: the effect of ZnO particle size on the adsorption performance. Appl. Catal. B **119–120**, 13–19 (2012)